Reprinted from

Symposium on

Machine Processing of

Remotely Sensed Data

June 3 - 5, 1975

The Laboratory for Applications of
Remote Sensing

Purdue University
West Lafayette
Indiana

IEEE Catalog No.
75CH1009-0 -C

SIGNATURES ANALYSIS AND RECOGNITION OF SEVERE WEATHER PATTERNS*

Paul P. Wang
University of Massachusetts
Amherst, Massachusetts and
Duke University, Durham, N. C.

Richard C. Burns
Duke University
Durham, N. C.

I. ABSTRACT

The results of observing the radiation from lightning discharge processes by William L. Taylor has indicated that radio frequency electrical activity was associated with the tornado-producing severe storms that struck Oklahoma City during April, 1970. This paper reports our findings as the result of analyzing Taylor's atmospherics rate data employing the techniques of time series analysis and pattern recognition. It shows the promise that sferics rate data can be used to establish unique signatures for the task of forecasting various severe weather patterns, however an extensive analysis of more data is needed before affirmative conclusions can be drawn.

II. INTRODUCTION

In this paper we intend to answer some of the questions concerning the feasibility of designing a prediction and warning system for severe weather conditions employing the techniques of time series analysis and pattern recognition. The problem is motivated by the steadily increasing massive computer applications in weather research and the promising experimental results obtained by researchers observing the major radio frequencies of electrical activities associated with severe storms.

To a large extent, most of the current knowledge on severe storm forecasting has been based on identifying the different characteristics of the severe weather through the mediums of radar and/or by satellite imagery. However, it is also known that a large majority of the various types of the severe weather encountered exhibit the common characteristic of electrical disturbances, called atmospherics, or simply sferics, and based on the recent research results of Taylor (1972), Hughes and Pybus (1972), and others, there is evidence indicating that an electronic detector capable of observing the rates of occurrence of atmospherics combined with modern data processing techniques will be able to do a better and faster job of forecasting and detecting the severe weather as compared to the conventional techniques presently in use.

The foundation of this research is based on atmospheric disturbances producing various electromagnetic signals containing certain characteristics identifiable to the type of storm which has generated them. Specifically, particular effort has been directed toward forecasting tornadoes (Taylor, 1972) in which these signals are referred to as the electromagnetic signature of the tornado. To examine this possibility Taylor has designed an experiment gathering sferics data during the Spring, 1970 tornado season in Oklahoma (Taylor, 1961), in which the rate of occurrence of sferics were observed by averaging the number of responses of a resonant circuit per unit of time at 5 amplitude levels for each frequency channel extending from the VLF into the VHF, the experimental set-up and the data obtained has been described in detail by Taylor (1973). This data forms the basis for our preliminary analysis and interpretation. Based upon one section of a season's data, we were able to show that the severe weather conditions indeed inherit their unique signatures respectively.

To be sure of no possibility of the duplication of this research with other efforts, more than two hundred documents have been collected, studied and classified into six topics, as shown in the Bibliography on Tornado Research (Wang and George, 1974). This report clearly indicates that the research being done in the detection and prediction aspect constitutes the least amount of effort (approximately 8.59%) in total research on tornadoes up to this date.

*This research work has been supported by a NASA research grant, NSG 5020.

The research has been carried out in the following three orderly stages: (1) Data Acquisition, (2) Data Preprocessing and Feature Extraction, (3) Severe Storms Recognition. The results of the third stage is the final goal and the first two stages are the pre-requisite for the third. However, only the findings of the first two stages will be reported here and the last stage of research constitutes the subject matter to be discussed in a followup paper.

III. DATA ACQUISITION

The data acquisition system in the context of our framework is somewhat different than the conventional systems where field or laboratory experiments are performed to acquire the data. Instead, our system involves the acquiring of data through the cooperation of Dr. William Taylor of ERL/NOAA, and what is meant by data acquisition, for our purposes, is the acquiring of data that will result in an effective analysis.

We have 55 figures of Taylor's 1970 Oklahoma data, obtained using his electronic tornado detector (Figure 1), supplied by him in photographic form. Based upon only one season's sferic rate data of severe storms, a total of 6 classes (patterns) of severe storms has been designated; (I) tornadoes, (II) decayed tornadoes, (III) lightning discharges, (IV) thunderstorms, (V) decayed thunderstorms, (VI) funnels and to each pattern above, 5 time series have been processed. To illustrate Figure 14 and 15 are the best examples of a tornado's sferic rate activity (Taylor, 1961) and characteristic of large bursts during the decaying state of a thunderstorm are shown in Figures 27 and 55 of reference (Taylor, 1961). However, a more complete classification has been suggested by Taylor (1973) as follows: (I) tornadoes, (II) thunderstorms, (III) hail, (IV) strong winds and (V) funnels. The above classification is possible because Taylor has incorporated more data since 1970 into his analysis.

By looking at data in our possession, we have decided to analyze the figures with the slow time constant, since the form that the data was received in (glossy pictures) did not permit high resolution in the analog-to-digital, (A/D), conversion of the fast time constant data. This A/D conversion up to the present time has been completed through the use of an automatic x-y position recorder, GRAF/PEN Science Accessories Corp., in conjunction with the Digital Equipment Corporation. PDP-11/45 computer. Our current data bank contains 108 time series in total which approximates the original series in digital form. Figures 2(a), 2(b), 3(a), and 3(b) show some of the digital time series using linear interpolation between the digitized points as reproductions of channel 16, Figure 6 (lightning discharge) and channel 16, Figure 15 (tornado) and also channel 28 of Figures 6 and 28, respectively.

IV. DATA PREPROCESSING AND FEATURE EXTRACTION

Since we do not have a large number of time series available from one generator (one channel of a particular storm) the assumption of ergodicity was made in our analysis of sferics rate time series of the severe weather. To put the sferics rate time series of a life cycle of a severe storm in perspective, we show in Figure 4 a simulated model consisting of the complete "birth" until "death" of a thunderstorm. As one can see in this illustration there are 5 discrete steps, in which the sferics rate up to time (t_a) is considered to be normal, in the interval (t_a) to (t_b) a time of pre-thunderstorm is occurring, this is when the forecasting of the storm should occur, then from (t_b) to (t_c) the thunderstorm occurs, (t_c) to (t_d) the period of post-thunderstorm is present, and beyong (t_d) the period of normal activity returns. As one may have noticed in this illustration several questions arise, that is: When do we choose the times t_a, t_b, t_c, and t_d? Is the process ergodic? Is the process stationary in some sense? We can not answer all these questions at this time because we do not have enough data to be analyzed. However, we are in a position now to state that one of the most violent land storms, the tornado, has exhibited, in the section of channel 28 of the time series of Figure 15, April 18, 1970 we have analyzed at least approximates a stationary process in a preliminary examination.

Since nature is the generator of the time series, it is unlikely that one time series will resemble another time series visually in the domain of time. Therefore, there is a problem of feature extraction from the time series data that will enable us to determine what time of severe weather, if any, is going to occur. We propose that the empirical time series analysis technique of Parzen (1965) and the familiar measurement of power spectra technique of Blackman and Tukey (1958) will be used as the main tools for extracting features from the sferics rate data. The following equations give a summary of the type of analysis that has been implemented by us in our preliminary study of the sferics rate data.

The sample mean for N samples of the digital data (x_i) is calculated as

$$\bar{X} = \frac{1}{N} \sum_{i=0}^{N-1} x_i$$

and the unbiased sample variance s^2 is obtained from

$$s^2 = \frac{1}{N-1} \sum_{i=0}^{N-1} (x_i - \bar{X})^2$$

The digital power spectral density may also be defined, according to Blackman and Tukey (1958), in two steps. First, the sample autocorrelation function is computed:

$$R_r = \frac{1}{N-r} \sum_{k=0}^{N-r-1} x_k \, x_{k+r}, \quad r = 0,1,2,\ldots,m.$$

The subscript r corresponds to the variable τ, lag. The second step consists of taking the cosine transformation of the autocorrelation function, which yields

$$G_p = \Delta t\ 2T_o + 4 \sum_{r=1}^{m} R_r \cos \frac{\pi p r}{m}$$

As pointed out by Otnes and Enochson (1972), the alternative is to use the Fourier transform and obtain

$$G_p' = \frac{1}{N\Delta t} X_q^* X_q = \frac{1}{N\Delta t} |X_q|^2,\ q = 0,1,2,\ldots,\ N$$

As $m \longrightarrow N$ and $N \longrightarrow \infty$, G_p and G_p' will approach each other.

As is well known, if one is seeking to estimate the spectral density functions of covariance stationary time series, one cannot use the sample spectral density function but must use windowed sample spectra (Blackman and Tukey, 1958). The computed spectral density matrix

$$\underline{g}(\omega) = \begin{vmatrix} g_{11}(\omega) & g_{12}(\omega) & \cdots & g_{1r}(\omega) \\ g_{21}(\omega) & g_{22}(\omega) & \cdots & g_{2r}(\omega) \\ \cdot & \cdot & & \cdot \\ \cdot & \cdot & & \cdot \\ \cdot & \cdot & & \cdot \\ g_{r1}(\omega) & g_{r2}(\omega) & & g_{rr}(\omega) \end{vmatrix}$$

where the diagonal element is called the spectral density function and the off diagonal element is called the cross-spectral density, has been proved to be a valuable tool in our analysis. In order to obtain specific numerical results, we have chosen the "Time Series Analysis," BMD02T Program of UCLA and it has been executed by the CDC Cyber 74 high speed computer. In addition to the essential concepts described above, the program also computes the phase shift between two time-series and their transfer function. The numerical results are satisfactory as shown in some sample plots such as in Figure 5 (power spectrum), Figure 6 (cross-covariance), and Figure 7 (coherence function of two time series). Extensive experiments have been carried out concerning the relationship between the accuracy of estimation and the choice of sampling frequency. It is worthwhile to mention here that numerous previous research works, other than weather research, have been carried out to tackle the problem of recognizing time series patterns. However, those families of time series often arise in the biomedical or seismic areas and present themselves quite a different problem, and time domain approaches were often used. In addition, we have found that the computation of coherence function is very useful. The concept of coherence, for example, between the series $X_j(\cdot)$ and $X_k(\cdot)$,

$$W_{jk}(\omega) = \frac{|g_{jk}(\omega)|^2}{g_{jj}(\omega)\ g_{kk}(\omega)}$$

is related to a frequency decomposition of the residual series when one uses either of the series $X_j(\cdot)$ and $X_k(\cdot)$ to predict the other (Parzen, 1965).

The task of classifying various severe storms can not be accomplished unless we can find unique signatures for each severe storm. However, the signatures are complicated enough that we need not one, but multiple features as well as an ingenious way of processing these features. So the problem all boils down to the success of extracting features satisfying some criteria.

Looking at the computer printouts, the estimated spectral and cross-spectral density functions all give a small number of distinct peaks occurring at several distinct frequencies. For comparison purposes, a threshold of 20 has been set on the amplitude of the peaks, which limits the amount of data entering the above mentioned estimated spectral density matrix. Features extraction has always been an important problem in pattern recognition research and many important aspects should be considered as described by Fu et al (1970). In this problem, the peaks of the spectral density function with different amplitudes occurring at distinct frequency components serve as our principle discriminant information for time series patterns. To complete the analysis of unique signatures of severe weather patterns, we put the data in a learning algorithm called (M,N) algorithm (Wang and Burns, 1974) to obtain the desired results.

IV. RESULTS AND INTERPRETATIONS

We have selected 30 time series from our data bank of 108 time series to be computed. These time series correspond to channel 4 (10 kHz, 10.0 v/m), channel 7 (31.6 kHz, 1.0 v/m), channel 8 (31.6 kHz, 3.16 v/m), channel 16 (316 kHz, 0.316 v/m) and channel 28 (3.16 MHz, 0.316 v/m) of Taylor's original data (Taylor, 1972) of Fig. 15 (class I, Tornado), Fig. 16 (class II, decayed tornado), Fig. 6 (class III, lightning discharge), Fig. 19 (class IV, thunderstorm), Fig. 27 (class V, decayed thunderstorm), Fig. 23 (class VI, funnel). However, only the computational results of channels 16 and 28 will be tabulated here in Tables I and II, without losing much of the generality in illustrating our proposed techniques of signatures analysis.

A. POWER SPECTRA

Table I tabulates the peaks (designated as with a positive derivative on the left and a negative derivative on the right of the power spectrum density graph) of the spectral density matrix above a threshold of 20. The time series appearing in the vertical direction represents the first one and those in the horizontal direction represent the second one in the cross-correlation.

By looking at the auto-power spectrum for class I, c28, one can see that 0.35 Hz is the only major frequency component, other than the d.c. Through further investigation of the remaining

auto-power spectrums of c28, one can note that class I, c28, is the only element that contains this 0.35 Hz component. Figure 8, a plot of the peaks of the auto-power spectrums, reconfirms this, but goes further in suggesting that the tornado has the highest first frequency component. It is interesting to note here that Taylor (1973) suggested that "... the parameter most indicative of tornadic activity is the number of bursts of high atmospherics rates at frequencies above about 1 MHz" can easily be verified from computer print-out in a very precise term as "one of the parameters most indicative of tornadic activity is the first frequency (number of bursts) of the spectral density, of high atmospherics rates at 3.16 MHz (channel 28 in Taylor's original data (1971), is 0.35 Hz which is higher than any other severe storm".

Also from Table I, we have noted that when class II, c16, is crossed with class II, c28, a unique frequency component arises for class II (a decayed tornado).

B. CROSS-POWER SPECTRA

Another set of important features for signatures analysis can be obtained from the estimation of cross-power spectra. The first row of Table I tabulates the peaks as a result of taking channel 28 of a tornado cross-correlated with all classes of channel 28. For comparison purposes, all the components above the threshold of 20 are plotted in Fig. 9 instead of just the peaks, the difference is even more striking. In the case of the tornado, there exists many more frequency components as the result of cross-correlation. If a standard mask of a tornado can be established and stored in the memory of a computer, the tornado can be un-mistakenly detected.

The existence of multiple channels from Taylor's data suggests that the cross-correlation can indeed take place between time series of two different channels. We have experimented by computing the estimated cross-power spectra of channel 16 of all classes with channel 28 of tornado (not shown in Table I, note that this is different as compared with the 7th row of Table I), and the results are plotted in Fig. 10. The features shown in Figure 10 are very distinct and they are not duplicated when the tornado time series of channel 28 is replaced by the severe storms other than the tornado. The 7th row appeared in Table I does single out the class of funnel because of a strong peak occurs at 0.20 Hz. Similarly, if channel 16 of all classes are cross-correlated with the funnel data of channel 28, the decayed thunderstorm (no other peak exists except the d.c. component) and the funnel (the lowest non-d.c. component at 0.10 Hz) could have been easily identified. In fact, the whole spectral density matrix of Table I contains important information.

C. COHERENCE FUNCTIONS

It remains an open question whether it is more informative to plot the coherence $W_{jk}(\omega)$ or the residual spectral density functions, (Parzen, 1965), but we have decided to compute the coherence square and some results are summarized in Table II. In the process of computation, there are numerous instants that the value of coherence square are not computable due to a negative or zero spectral estimate or too high due to a sampling error. The occurrence of these phenomena reflects the violation of some assumed properties for some time series, nevertheless, Table II provides interesting information. It becomes quite clear by inspecting Table II that the behavior of a decayed thunderstorm is the most unpredictable case as compared with all others, followed by the cases of thunderstorm and funnel with much lesser degree. Relatively speaking, the classes of tornado, decayed tornado and lightning discharge are much more similar in nature. The above observation can even be confirmed visually by inspection if these corresponding time series were displayed from our data bank.

D. TIME-VARYING PATTERNS

It becomes obvious from Taylor's data that weather phenomena is a dynamic process. Hence the analysis of the sferic rate data for various stages, shown in Fig. 4, of the formation, especially the relationships among them, becomes very important. Unfortunately, the very limited one season's data does not provide enough data base for the analysis of thes kind especially when Taylor's original data supplied to us were available only in unconnected sectional pieces. However, we were able to make some isolated observations; (1) the sferics rate time series of a tornado behaves quite differently at the peak of activity and after the peak (Table I) where the decayed tornado has a much wider bandwidth, but the form of the series does not vary drastically (Table II). (2) the magnitude of sferics activity reduces considerably after a thunderstorm is decayed (Table I). (3) obviously, the thunderstorm process inherits extremely high sferics activity where the level of activity decreases considerably in the decayed period.

V. CONCLUDING REMARKS

No affirmative conclusion can be drawn at this time because we have analyzed only a single season's data taken at a specific geographical location, but the analysis provides a sound ground for understanding the nature of the problem. We are not in a position to recommend a complete prediction and detection model unless we are willing to make a number of assumptions which have not been fully tested yet. However, it is not unrealistic at all to look into some working mathematical models for the purpose of signatures identification and recognition of severe storms. These results will be presented in a forthcoming paper. It seems safe to postulate that most features will be present in any severe storms but not all of the features in every occurrence. It is possible to build a detector taking a probabilistic situation into consideration. In fact, one can construct a system in a manner where the decision is reached only when the reenforcement with repeated verifica-

tion can be established. The selection of features has been discussed before and the proposed models based upon the learning of features can be achieved. The powerful linguistic approach which provides all possible combinations of features for a finite number of patterns, has been proven to be an invaluable tool for time varying pattern classification.

In conclusion, the time series analysis and pattern recognition techniques can be proven to be very attractive and useful methods in the study of weather patterns, and in order to build a practical prediction and warning system, much more sferics rate data must be analyzed. We feel strongly that the study of sferics rate data shows real promise for building a forecasting system capable of providing useful information a priori to the occurrence of a severe storm.

ACKNOWLEDGMENT

The authors would like to express their thanks to William L. Taylor of NOAA for providing his experimental data and stimulating discussions during the course of the research.

REFERENCES

1. Taylor, W. L., "Atmospherics and Severe Storms," Remote Sensing of the Troposphere, edited by V. E. Derr, Chapter 17, U.S. Government Printing Office, Washington, D.C., 1972.

2. W. L. Hughs and E. J. Pybus, "Severe Storm Sferics-Stroke Rate," Proc. 14th Radar Meteorology Conference, Tucson, Arizona, 1970, pp. 315-318.

3. Dinger, H. E., "Report on URSI Commission IV-Radio Noise of Terrestrial Origin," Proc. IEEE, Vol. 46, No. 7, July 1958.

4. Taylor, W. L., "Evaluation of an Electromagnetic Tornado-detection Technique," Proc. 8th Conference on Severe Local Storms, AMS, Boston, Massachusetts, October 1973, p. 4.

5. Taylor, W. L., "Review of Electromagnetic Radiation Data from Severe Storms in Oklahoma during April 1970," NOAA Technical Memorandum, ERL WPL-6, June 1971.

6. Taylor, W. L., "Electromagnetic Radiation from Severe Storms in Oklahoma during April 29-30, 1970," Journal of Geophysical Research, Vol. 78, No. 36, December 20, 1973.

7. Taylor, W. L., "An Electromagnetic Technique for Tornado Detection," Weatherwise, Vol. 26, No. 2, April 1973, pp. 70-71.

8. Hughes, W. L., P. A. McCollum, E. J. Pybus, and E. L. Shreve, "A Center for the Description of Environmental Conditions Weather Phenomena," Final Report, Project Themis, Oklahoma State University, ECOM-0083-14, September 1973.

9. Wang, P. P. and R. T. George, Jr., Bibliography on Tornado Research, TR-74-01, Department of Electrical Engineering, Duke University, August 1974.

10. Otnes, R. K. and L. Enochson, Digital Time Series Analysis, John Wiley and Sons, New York, 1972.

11. Parzen, E., "On Empirical Multiple Time Series Analysis," Proc. of the Fifth Berkeley Symposium on Mathematical Statistics and Probability, June and December 1965, University of California Press, pp. 305-340.

12. Blackman, R. B., and J. W. Tukey, The Measurement of Power Spectra from the Point of View of Communications Engineering, New York: Dover, 1958.

13. Fu, K. S., P. J. Min, and T. J. Li, "Feature Selection in Pattern Recognition," IEEE Trans. on Systems Science and Cybernetics, SSC-6, No. 1, January 1970, pp. 33-39.

14. Wang, Paul P., and R. C. Burns, "Optimal Features Selection Algorithm for a Binary-Partitioned Classification Scheme," Proceedings, 12th Annual Allerton Conf. on Circuit and System Theory, Univ. of Ill., October 1974, pp. 288-297.

channel 28 / channel 28 and 16	class I c 28	class II c 28	class III c 28	class IV c 28	class V c 28	class VI c 28
class I c 28	0.00 Hz; 54.8 0.35 Hz; 35.6	—	0.00 Hz; 20.1	0.05 Hz; 35.2	—	0.00 Hz; 38.6
class II c 28		0.00; 52.4 0.15; 33.0 0.40; 33.3 0.50; 26.8	0.00; 22.1	—	—	0.00; 45.9
class III c 28			0.00; 64.1 0.15; 40.0 0.40; 39.2	—	—	0.00; 34.4
class IV c 28				0.00; 309.2	0.00; 109.9	0.00; 54
class V c 28					0.00; 72.0	0.00; 24.2
class VI c 28						0.00; 94.8 0.25; 83.0 0.55; 28.1
class I c 16	0.00; 22.3	0.00; 23.0	0.00; 28.9	0.10; 33.7	—	0.00; 24.7 0.20; 29.2
class II c 16		0.05; 31.0	—	0.00; 61.0 0.15; 22.5	0.00; 23.8	0.20; 31.9 0.30; 38.9
class III c 16			—	0.10; 33.7	—	0.00; 24.7 0.20; 29.2
class IV c 16				0.00; 150.7 0.10; 65.7	0.00; 83.0	0.00; 68.4 0.20; 46.4 0.30; 31.0
class V c 16					0.00; 97.7	0.00; 80.3
class IV c 16						0.00; 23.1 0.10; 32.6

Remarks: The first number represents frequency component in Hz; the number underlined denotes the peaks amplitude above 20.

Table I: Tabulation of the peaks of the spectral density matrix.

channel 28 / channel 28 and 16	class I c 28	class II c 28	class III c 28	class IV c 28	class V c 28	class VI c 28
class I c 28		—	—	— x **	5.0 Hz; 0.81 x **	—
class II c 28			—	— x **	2.25; 1.00 2.65; 1.00 3.15; 0.98 3.50; 1.00 x **	—
class III c 28				0.90; 1.00	2.45; 1.00 3.65; 0.98 x **	—
class IV c 28	x : At least one value is not computable due to a negative or zero spectral estimate				— x **	0.95; 1.00 x
class V c 28	** : At least one value is too high due to sampling error.					3.0; 0.84 x
class VI c 28						
Class I c 16	—	—	—	— x	2.35; 0.91 2.85; 0.85 3.45; 0.87 x **	—
class II c 16	—	—	—	—	1.75; 0.82 2.00; 0.86 3.25; 0.91 4.00; 0.84	—
class III c 16	—	—	—	0.90; 1.00	2.35; 0.90 2.85; 0.85 3.45; 0.87	—
class IV c 16	3.05; 0.92	—	—	— x	0.30; 0.98 1.95; 1.00 3.75; 0.92 4.05; 0.88 x **	2.90; 0.94 3.05; 1.00 3.40; 0.90 3.60; 0.98
class V c 16	—	—	—	— x **	**	—
class VI c 16	—	—	3.45; 0.98	— x **	4.70; 0.95	—

Remark: The data shown denotes the peaks of the coherence square (underlined) above 0.80 at frequency components in Hz.

Table II: Tabulation of the peaks of the coherence function of two time series.

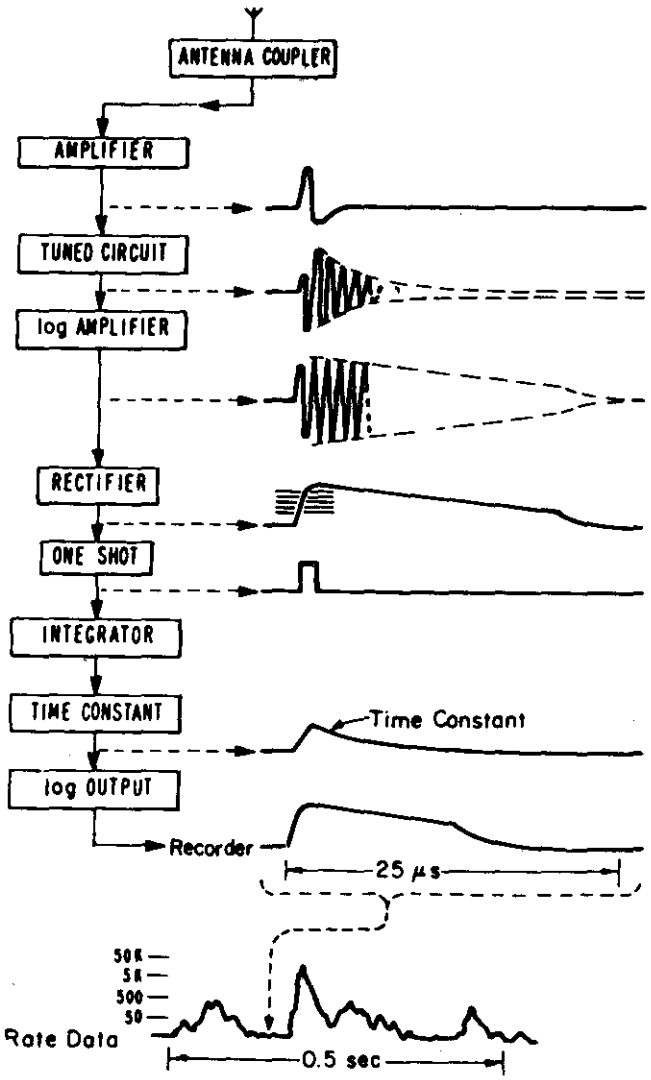

Fig. 1. Simplified block diagram and circuit responses for atmospherics rate equipment.

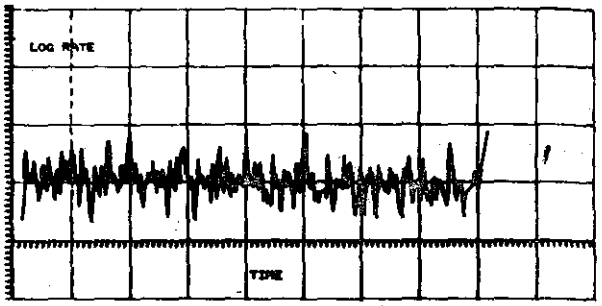

FIGURE NUMBER 15 CHANNEL NUMBER 16
TOTAL NUMBER OF POINTS TAKEN 478
TOTAL TIME 114.0
MAXIMUM RATE MEASURED IN K HERTZ
MINIMUM RATE MEASURE IN HERTZ
MAXIMUM RATE 1.6 MINIMUM RATE 16.0
0

Figure 2(a) A sample time series from data bank, Fig. 15, channel 16.

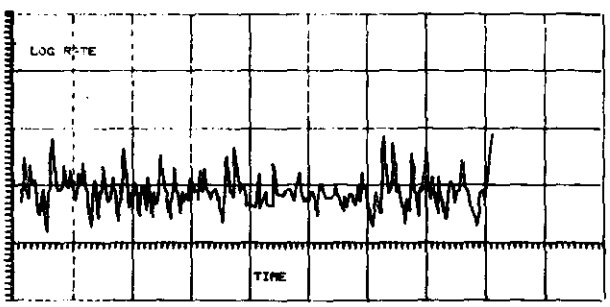

FIGURE NUMBER 06 CHANNEL NUMBER 16
TOTAL NUMBER OF POINTS TAKEN 362
TOTAL TIME 114.0
MAXIMUM RATE MEASURED IN K HERTZ
MINIMUM RATE MEASURE IN HERTZ
MAXIMUM RATE 1.6 MINIMUM RATE 16.0

Figure 2(b) A sample time series from data bank, Fig. 6, channel 16.

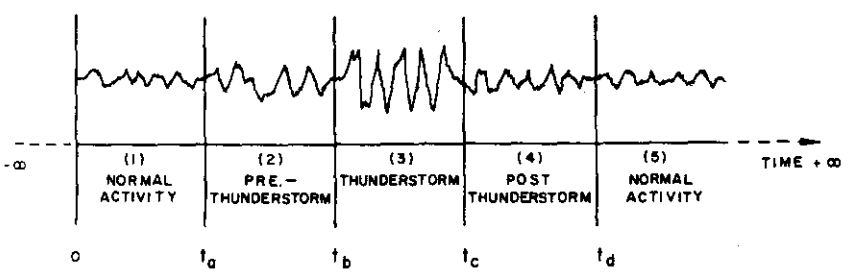

Figure 4 The life cycle of a thunderstorm.

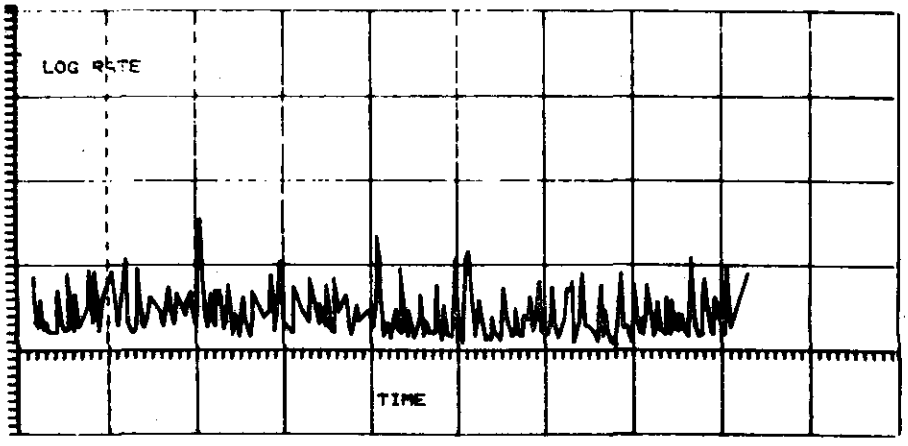

FIGURE NUMBER 15 CHANNEL NUMBER 28
TOTAL NUMBER OF POINTS TAKEN 290
TOTAL TIME 114 0
MAXIMUM RATE MEASURED IN K HERTZ
MINIMUM RATE MEASURE IN HERTZ
MAXIMUM RATE 1 6 MINIMUM RATE 0 0

Figure 3(a) A sample time series from data bank, Fig. 15, channel 28.

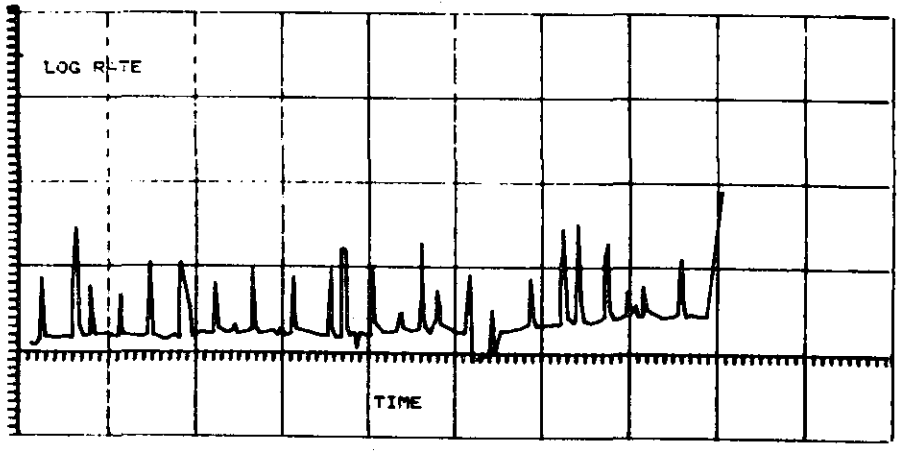

Figure 3(b) A sample time series from data bank, Fig. 6, channel 28.

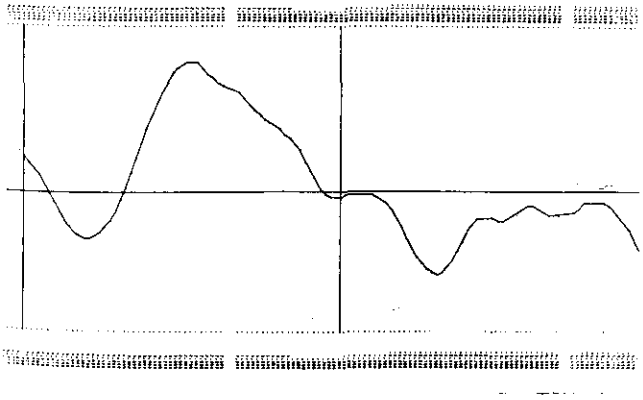

Figure 6 A sample cross-covariance.

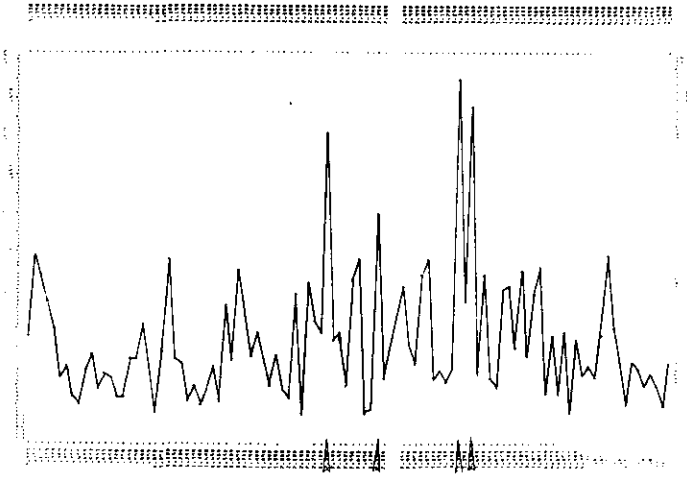

Figure 7 A sample of coherence function of two time series.

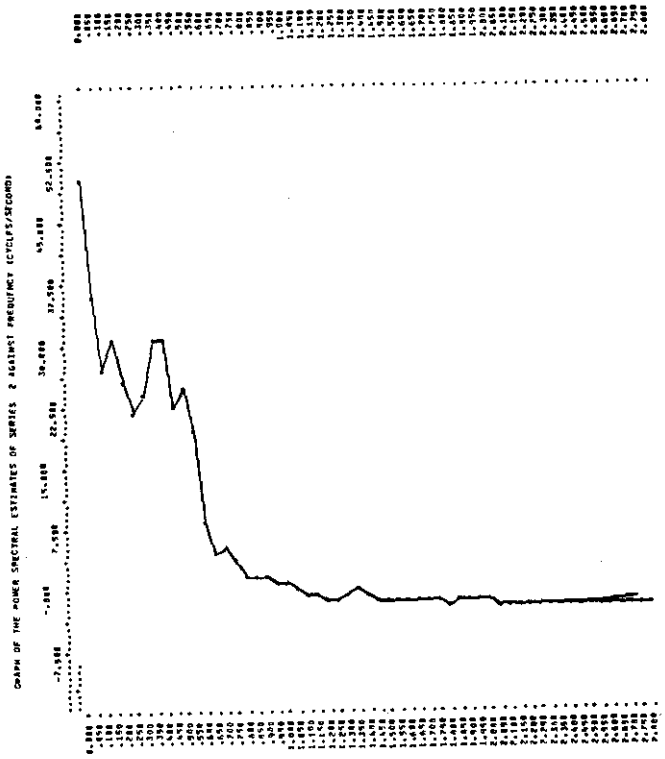

Figure 5 A sample power spectrum.

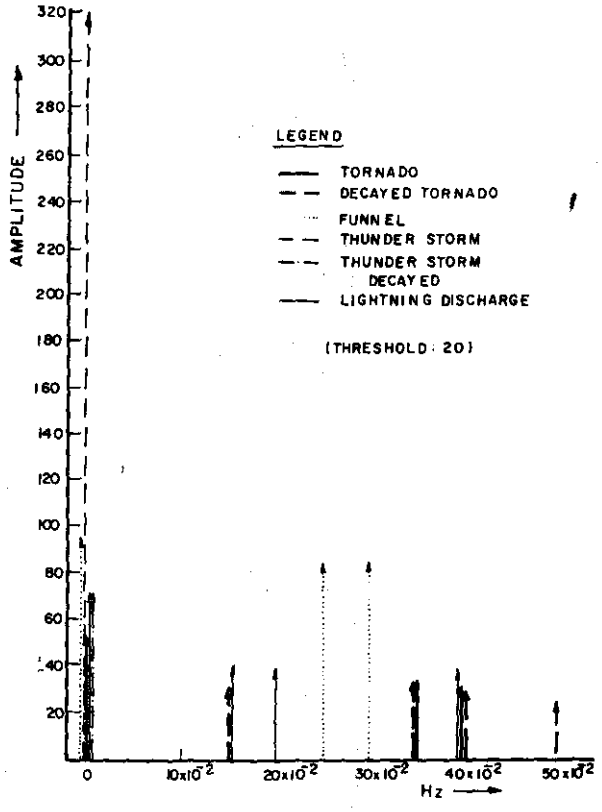

Figure 8 Distinct peaks at discrete frequencies of the power spectra of channel 28 for various severe storms.

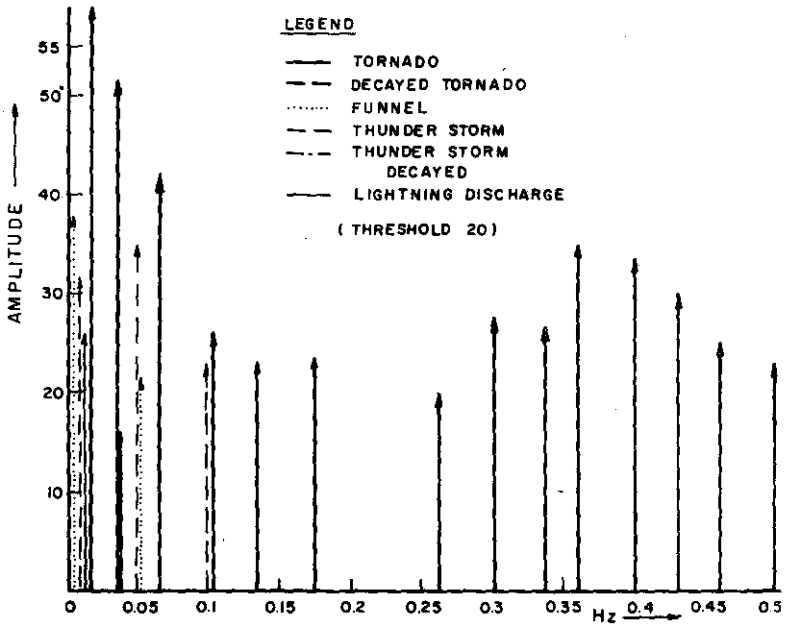

Figure 9 A proposed cross-correlator for time series from the same channel.

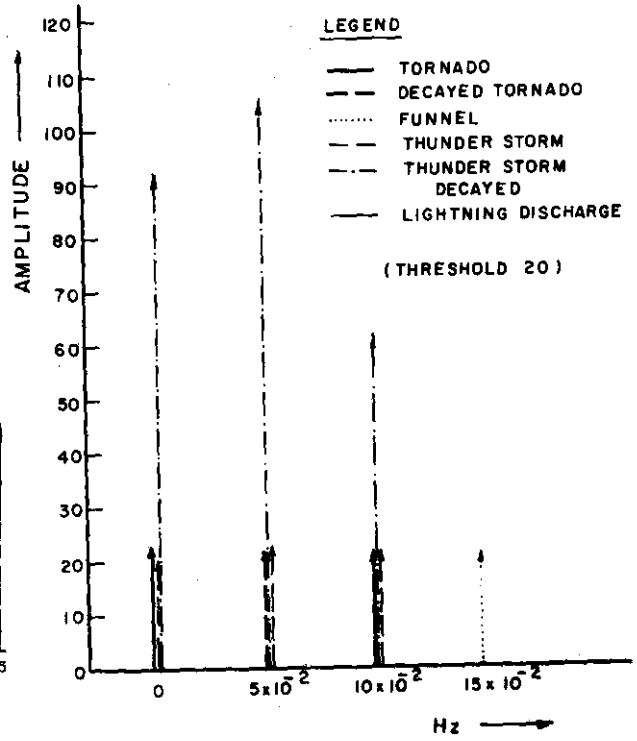

Figure 10 The result of tornado time series (channel 28) cross-correlated with all classes of channel 16.